Materials Science & Engineering A 652 (2016) 1–6

Contents lists available at ScienceDirect

Materials Science & Engineering A

journal homepage: www.elsevier.com/locate/msea

Improving the high-temperature creep strength of 15Cr ferritic creep-resistant steels at temperatures of 923–1023 K

M. Shibuya*, Y. Toda, K. Sawada, H. Kushima, K. Kimura

National Institute for Materials Science, Sengen 1-2-1, Tsukuba, Ibaraki 305-0047, Japan

ARTICLE INFO

Article history:
Received 11 September 2015
Received in revised form
20 November 2015
Accepted 22 November 2015
Available online 23 November 2015

Keywords:
Ferritic steel
Creep-resistant steel
Creep strength
Nickel
Precipitation
Microstructure

ABSTRACT

The precipitation strengthening of creep-resistant 15Cr ferritic steels at temperatures of 923–1023 K was improved by nickel addition. The addition of nickel, an austenite-stabilizing element, enhanced the formation of martensitic grains in the ferritic grain boundaries and changed the precipitation behavior during creep at elevated temperatures. The precipitates produced in the creep-ruptured 15Cr steels were intermetallic compounds (Laves phase and χ-phase), carbide ($Cr_{23}C_6$), and Z phase (Cr(V,Nb)N). An increase in the amounts of intermetallic compounds and the preferential precipitation of $Cr_{23}C_6$ carbide on the grain boundaries between the ferritic and martensitic grains were accelerated by the nickel addition. The 15Cr steel after 10,000 h at 973 and 1023 K demonstrated approximately double the creep rupture strength of 9Cr steel (ASME Grade T92) with a tempered martensitic microstructure. At temperatures of up to 1023 K, the 15Cr steel had over 10 times the creep rupture lifetime of T92 steel, primarily because of increased precipitation of intermetallic compounds and $Cr_{23}C_6$ carbide enhanced by nickel addition.

1. Introduction

High function steels with high thermal resistance have recently become highly desirable for eco-energy and CO_2 reduction regulation. Ferritic steels with a high chromium content have been found to have improved properties such as thermal conductivity, thermal expansion coefficient, oxidation resistance, and creep resistance [1]. The amount of chromium in ferritic steels must be limited to less than approximately 12 mass% in order to avoid the formation of δ-ferrite, which is a detrimental phase that reduces creep strength and fracture toughness. This chromium content limitation makes the simultaneous improvement of both long-term creep strength and oxidation resistance difficult. Therefore, ferritic steels with 9–12% Cr addition were developed, and steels with a tempered martensite microstructure were strengthened by numerous carbide and MX carbonitride precipitates [2–6]. The 9–12%Cr ferritic steels have already been used extensively for large components in ultra-supercritical (USC) power plants with operating temperatures of 873 K. However, 9–12% Cr ferritic steels undergo microstructural degradation during long-term creep exposure at high temperatures due to preferential recovery in the vicinity of prior austenite grain boundaries, and this phenomenon results in reduced creep strength [7].

Recently, the creep strength and toughness of solution-treated 15Cr ferritic steels with low dislocation densities have been improved by the addition of tungsten, cobalt, and nickel through precipitation strengthening effects [8–16]. The mechanical properties of 15Cr ferritic steels at elevated temperatures are strongly influenced by the precipitation of intermetallic compounds and carbides. The addition of nickel, which is an accelerator of martensite phase precipitation, has a particularly strong influence on precipitation behavior. In the present work, the effect of nickel addition on the precipitation strength of 15Cr steels was investigated at temperatures of up to 1023 K.

2. Experimental procedure

Test steel, which has a chemical composition of 15Cr–*x*Ni–2Co–1Mo–6W–0.05C–0.2V–0.06Nb–0.2Si–0.04N–0.003B (mass%), as shown in Table 1, was melted in a vacuum induction furnace. A 50 kg ingot of the test steel was hot-rolled to produce a 15-mm-thick plate, which was then solution treated for 30 min at 1473 K followed by water quenching. The creep test specimen had a 6 mm gauge diameter and a 30 mm gauge length, according to Type 14A of the Japanese Industrial Standard (JIS) Z 2201 [17]. The creep tests were conducted from 923, 973, and 1023 K in air, over a range of stresses from 30 to 300 MPa. The creep strain was measured using an extensometer attached to the gauge portion of the specimen. The Vickers hardness of creep-ruptured 15Cr steel was measured under a load of 49 N. Thermodynamic calculation software (Thermo-Calc) was used to predict the type and amount of

* Corresponding author.
E-mail address: SHIBUYA.Masachika@nims.go.jp (M. Shibuya).

http://dx.doi.org/10.1016/j.msea.2015.11.068
0921-5093/

Table 1
Chemical compositions of 15Cr steels (mass%).

	C	Cr	Ni	Co	Mo	W	V	Nb	N	B
0.8Ni	0.051	15.16	0.86	1.96	1.03	6.03	0.21	0.06	0.037	0.0031
1.4Ni	0.048	15.13	1.41	1.99	1.03	6.02	0.21	0.058	0.037	0.0031
2.1Ni	0.051	15.07	2.15	2.04	0.98	6.03	0.21	0.054	0.036	0.0031

precipitates in the test steel at elevated temperatures. The precipitates were identified by X-ray diffraction (XRD) analysis and inductively coupled plasma (ICP) atomic emission spectrometry of electrolytically extracted residues obtained from the creep-ruptured steels. The microstructures of the creep-ruptured specimens were observed by scanning electron microscopy (SEM) and scanning transmission electron microscopy (STEM) using carbon extraction replicas. Elemental analysis of the precipitates in the creep-ruptured specimens was carried out using energy-dispersive X-ray spectrometry (EDS).

3. Results and discussion

The addition of nickel to solution treated 15Cr steels formed two-phase ferritic and martensitic phases. Fig. 1 shows optical micrographs of the solution-treated 15Cr steels. The volume fraction (V_f) of the martensite phase is indicated in each micrograph. The addition of nickel, an austenite stabilizing element, resulted in a two-phase microstructure consisting of ferrite grains (white contrast) with a martensite phase (gray contrast) along the grain boundaries of the coarse ferrite grains. The ferrite grain size decreased with increasing nickel addition, and the V_f values for the martensite phase increased with increasing nickel content.

The creep rupture strengths of 15Cr steels with various nickel contents at 923, 973, and 1023 K are shown in Fig. 2. The creep rupture curves for 9Cr–0.5Mo–1.8W–V–Nb steel (ASME T92, a conventional ferritic heat-resistant steel with a tempered martensitic microstructure that has the highest creep strength of the ferritic steels used in modern thermal power plants [18]), was included for comparison (dashed line). The arrow in this figure indicates the sample from which a measurement result has not been obtained yet. The creep rupture lifetimes of the 15Cr steels at 973 and 1023 K were approximately 100 times those of the T92 steel, but at measurement temperatures lower than 50 K the lifetimes of the 15Cr steels corresponded well to those of the T92 steel. The creep strength of the 15Cr steel after 10,000 h at 973 K was almost double that of the T92 steel. The curve slopes for the 15Cr steels and T92 steel were almost the same just before rupture. The creep rupture lifetimes of the 15Cr steels above 973 K clearly increased with increasing nickel content. The addition of

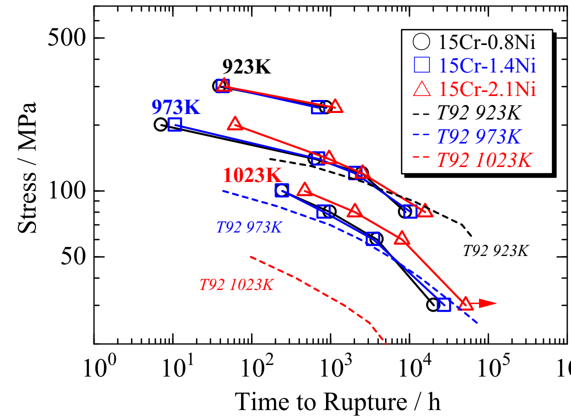

Fig. 2. Creep rupture strength of 15Cr steels with various Ni contents compared with a conventional heat resistant steel (ASME T92, dashed line) at 923, 973, and 1023 K.

nickel to the conventional 9Cr–8Mo steel [19] and the 15Cr–3Co steel [13,14] had a negligible effect on creep strength at 923 K. Moreover, increasing the nickel content to 1 wt% in 10Cr–2Mo steel at 973 K improved the rupture strength, but the high nickel addition led to decrease in effect on the precipitations [20]. This was probably caused by a decrease in the transformation temperature, which accelerated the recovery of the martensite matrix and negative precipitation behavior.

Creep rate versus time curves for 15Cr steels with various nickel contents at 923, 973, and 1023 K are shown in Fig. 3. The curve for T92 steel at 973 K under 120 MPa inserted in Fig. 3(b). The creep rate for 15Cr steels was lower than that for T92 steel from the initial stage of creep deformation. The minimum creep rate for 15Cr steels under the same conditions was a value of 1/1000, compared with that of T92 steel. The creep rate curves for all of the 15Cr steels indicated simple creep behavior, changing from transient creep to accelerating creep without a pronounced steady state creep stage. The onset time for the accelerating creep stage and the creep rupture lifetimes tended to increase with increasing nickel content. The effect of nickel addition was remarkable at 1023 K under 60 MPa.

The Vickers hardness of creep-ruptured 15Cr steels is shown in Fig. 4. The hardness of the creep-ruptured 15Cr steels was higher than that of the solution treated 15Cr steels. The hardness decreased with increasing creep rupture time. On the other hand, the hardness increased with increasing nickel addition. Thus, the dependence of the creep rupture time and nickel addition on the hardness, as same as the creep strength, is achieved.

Fig. 5 shows SEM micrographs (backscattered electron images) of 0.8Ni and 2.1Ni 15Cr steels, creep-ruptured at 923 K under 240 MPa, 973 K under 120 MPa, and 1023 K under 60 MPa. The

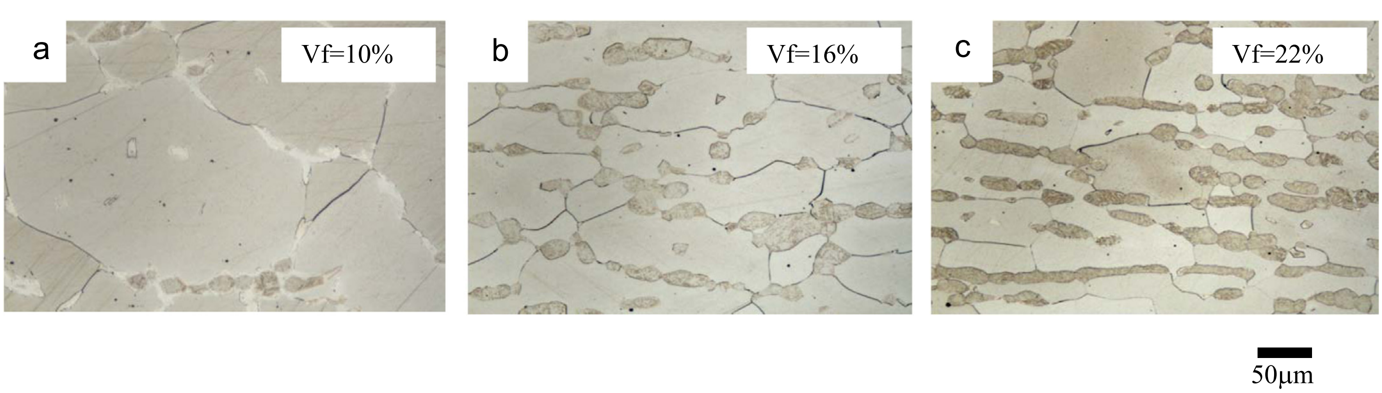

Fig. 1. Optical micrographs of 15Cr steels containing (a) 0.8Ni, (b) 1.4Ni, and (c) 2.1Ni after solution treatment for 30 min at 1473 K.